Electronic Supplementary Material (ESI) for Lab on a Chip.

Supplementary information to

On-chip electromagnetic tweezers - 3-dimensional particle actuation using microwire crossbar arrays

Philipp Rinklin[a,b], Hans-Joachim Krause[a], and Bernhard Wolfrum[a,b]

[a]Institute of Bioelectronics (ICS-8/PGI-8), Forschungszentrum Jülich, 52425 Jülich, Germany

[b]Fachgebiet Neuroelektronik, Fakultät für Elektrotechnik und Informationstechnik, Technische Universität München, Boltzmannstraße 11, D-85748 Garching

1 Local minimum in the electric field generated by four microwires

The electric fields generated by four microwires with relative amplitudes of 1, -0.75, 0.75, and -1 exhibit a local minimum at a height of approximately $z = 8\,\mu\text{m}$ (compare Fig. 2d). This effect can be explained as follows. Figure S1a shows a plot of the equipotential lines of an electric quadrupole composed of four charges of magnitude $\pm q = \pm 1.602 \times 10^{-19}\,\text{C}$. For symmetry reasons two lines corresponding to a potential of 0 V coincide with the axes of the coordinate system. At the origin of the coordinate system, these two lines meet under an angle of 90°. This leads to the local gradient of the potential (i.e. the electric field) being zero at this point. Moving the four charges diagonally towards the x-axis of the system as indicated by the arrows results in the potential distribution shown in Figure S1b. It can be seen that the horizontal zero-potential line is deformed. At the crossing point, however, both zero-potential lines still meet under a 90° angle leading to an electrical field of zero at this point. Extending this concept to a linear arrangement of charges leads to the potential distribution displayed in Figure S1c. In this case, the equipotential line forms a closed loop and the local minimum can be found over and under the charges.

In comparison, Figure S1d shows the equipotential plot corresponding to Figure 2d. While the geometry of the field lines is distorted due to the wires' rectangular shape and the step in the dielectric constant at $z = 0$ (see Methods section for simulation details), a crossing point of two zero-potential lines can still be found. Since, for symmetry reasons, both equipotential lines still meet under a right angle, the electric field at this point is zero.

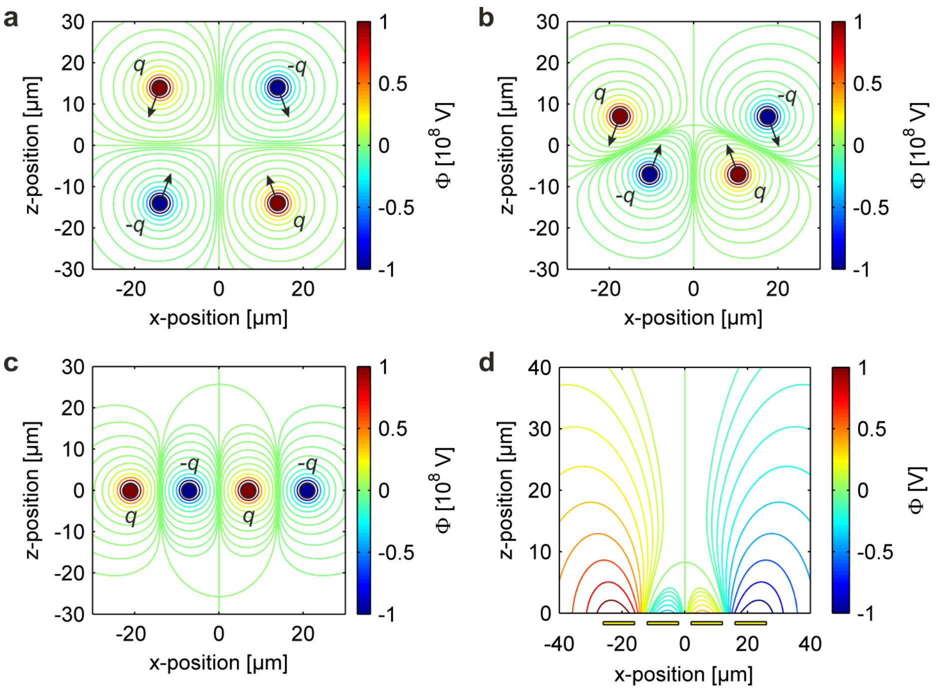

Figure S1: Potential distributions of various arrangements of line charges and micro-wires. **(a)** The equipotential plot of an e-lecÂňtric quadrupole displays two zero-potential lines that coincide with the coordinate axes. **(b)** Deforming the quadrupole as indicated by the arrows in **(a)** leads to a deformation of the horizontal quadrupole. **(c)** Further deformation to a linear arrangement leads to a closed loop for this equipotential line. At the crossing point of both zero-potential lines, however, the electric field remains zero. **(d)** Potential distribution corresponding to the electric field in Figure 2d. The geometry of the field lines is distorted by the wires' shape and the step in dielectric constant at $z = 0$. The crossing point of the two zero-potential lines can be found at approx. $z = 8\,\mu\text{m}$.

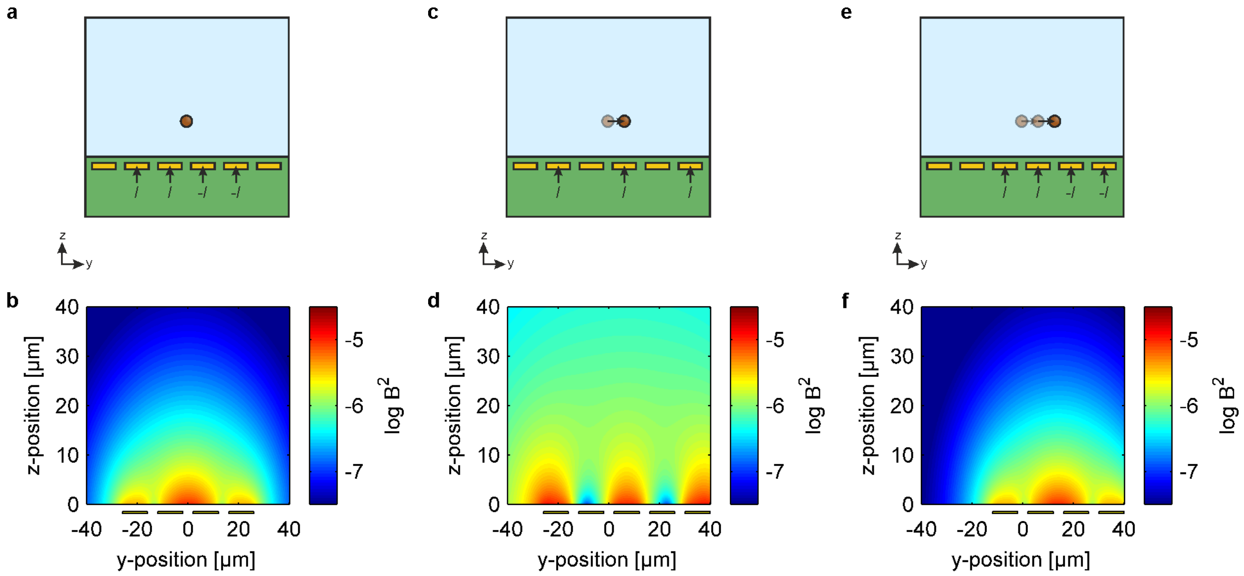

Figure S2: Schematics and simulated squared magnetic fields during the vertical switching protocol with an intermediate step. **(a)** During the first step of the protocol, four wires surrounding the particle are supplied with currents of I, I, $-I$, and I. **(b)** Simulated squared magnetic field for $I = 40\,\mathrm{mA}$. At a given z-height, the magnetic field exhibits a maximum at $y = 0$ trapping the particle at this position (as indicated in **(a)**). **(c)** During the intermediate step, five wires are supplied with relative amplitudes of I, 0, I, 0, and I. **(d)** Corresponding plot of the squared magnetic field. While the magnetic field shows three local maxima at a given z-height, the maximum at $y = 7\,\mu\mathrm{m}$ is closest to the particle's position at the beginning of this step. The particle is thus attracted towards this position (as indicated in **(c)**). **(e)** and **(f)** Activating a configuration analogous to the one shown in **(a)** completes the particle transfer.

2 Detailed description of the switching protocols

2.1 Switching protocols without intermediate steps

In order to transfer a particle from one position in the array to another during levitation, direct transitions between two corresponding traps were tested. In the case of a vertical translocation of the particle (i.e. parallel to the y-axis), this corresponds to directly switching from the configuration displayed in Figure S2a and b to the one displayed in Figure S2e and f. Similarly, in the case of a horizontal translocation of the particle, a direct switching protocol corresponds to an immediate transition from the configuration described in Figure S3a and b to that described in Figure S3e and f. In both cases, however, the transport suffered from poor reliability. In addition to the particle being lost a significant amount of times, it notably changed its z-height during successful jumps. Our previous work on reliable 2-dimensional particle transport at the chip's surface[1,2] indicated that subdividing the individual actuation steps can be used to address similar issues. Hence, switching protocols using an intermediate step were developed.

2.2 Vertical switching protocol with an intermediate step

Figure S2 shows schematics and simulated magnetic fields for the vertical switching protocol (i.e. along the y-axis) with an intermediate step. In this direction, the particle's position with respect to the upper set of wires is not changed. Consequently, the configuration of the AC signals applied to these wires remains constant during the switching procedure. Figure S2a shows a schematic of the initial configuration of a set of four wires

[1] Rinklin, P., Krause, H.-J. & Wolfrum, B. On-chip control of magnetic particles. *Phys. Status Solidi* **209**, 871âĂŞ874 (2012)
[2] Rinklin, P., Krause, H.-J. & Wolfrum, B. Actuation and tracking of a single magnetic particle on a chip. *Appl. Phys. Lett.* **100**, 014107 (2012).

used to generate a trap at a given point above the array. The two wires left and right of the particle are supplied with relative currents of I, I, $-I$, and $-I$, respectively (compare Fig. 2e). Figure S2b shows the squared magnetic field for $I = 40\,\mathrm{mA}$. The positions of the active wires are indicated by the yellow rectangles. At a given z-height, the maximum of the magnetic field is located at $y = 0$. In order to partially relocate the particle in the intended direction of movement, a DC configuration as indicated in Figure S2c is activated. In this configuration, five wires (with the wire to be crossed in the middle) are supplied with relative currents of I, 0, I, 0, and I. The resulting magnetic field is shown in Figure S2d with the active wires' position indicated by the yellow rectangles (simulation for $I = 65\,\mathrm{mA}$). In a given plane off the chip's surface, the magnetic field exhibits three local maxima. At the particle's location at the beginning of this step ($y = 0$), the gradient of the squared magnetic field, and thus the magnetophoretic force, points towards the maximum at $y = 7\,\mu\mathrm{m}$. The particle is thus moved to a position over the center of the wire to be crossed (compare Fig. 5c). Finally, activating a configuration analogous to the one in Figure S2a but shifted about one wire completes the particle actuation.

The above mentioned increase in the DC current per wire during the intermediate was used to keep the particle's levitation height constant during the jump. This is due to the fact that the gradient of the squared magnetic field with respect to the z-axis, and thus the magnetic force in this direction, is significantly weaker during this step (compare Figs. S2b and d). As the AC signals are kept constant, an increased DC amplitude is needed to keep the particle's levitation height constant.

Using the above described protocols, we were able to move levitating particles on the array without particle loss. The maximum switching frequency was 1 Hz, which corresponds to the particle being moved by one position in the array every 2 s.

2.3 Horizontal switching protocol with an intermediate step

Figure S3 shows schematics and simulated squared electric fields for the horizontal switching protocol (i.e. along the x-axis) with an intermediate step. When being moved along the x-axis only, the particle's position with respect to the lower set of wires remains constant. Thus only the configuration of the AC signals applied to the upper set of wires is changed during this protocol. Figure S3a and b show a schematic of the initial configuration of the AC signals used to generate a trap at a given position in the array, as well as a simulation of the corresponding squared electric field (respectively; simulation for a peak-to-peak input amplitude of 15 V, active wire positions indicated by the yellow rectangles). As discussed in the main text and above, the electric field of this configuration exhibits a local minimum in the center of the four wires. Consequently, the particle is dielectrophoretically trapped at this position. In order to move the particle to an intermediate position between the initial and target state, a configuration as depicted in Figure S3c was used. In this configuration an additional wire to the left of the particle is supplied with an AC signal of reduced amplitude. The resulting electric field distribution can be seen in Figure S3d (simulated for a peak-to-peak input of 15 V, active wire positions indicated by the yellow rectangles). Due to the contribution of the additional wire, the local minimum in the electric field is shifted towards the right and upwards, relocating the particle as indicated in Figure S3c. Due to the local minimum's change in z-height, the DC current applied to the lower wires was increased to 60 mA per wire in order to maintain a constant levitation height. Finally, the activation of a configuration analogous the one shown in Figure S3a and b, but shifted by one wire, is activated to complete the transfer (see Figure S3e and f). Using this protocol, we were able to reliably move levitating particles along the x-axis of the system. Similar to the above described vertical switching, the maximum actuation rate was found to be 0.5 Hz (i.e. one jump every 2 s).

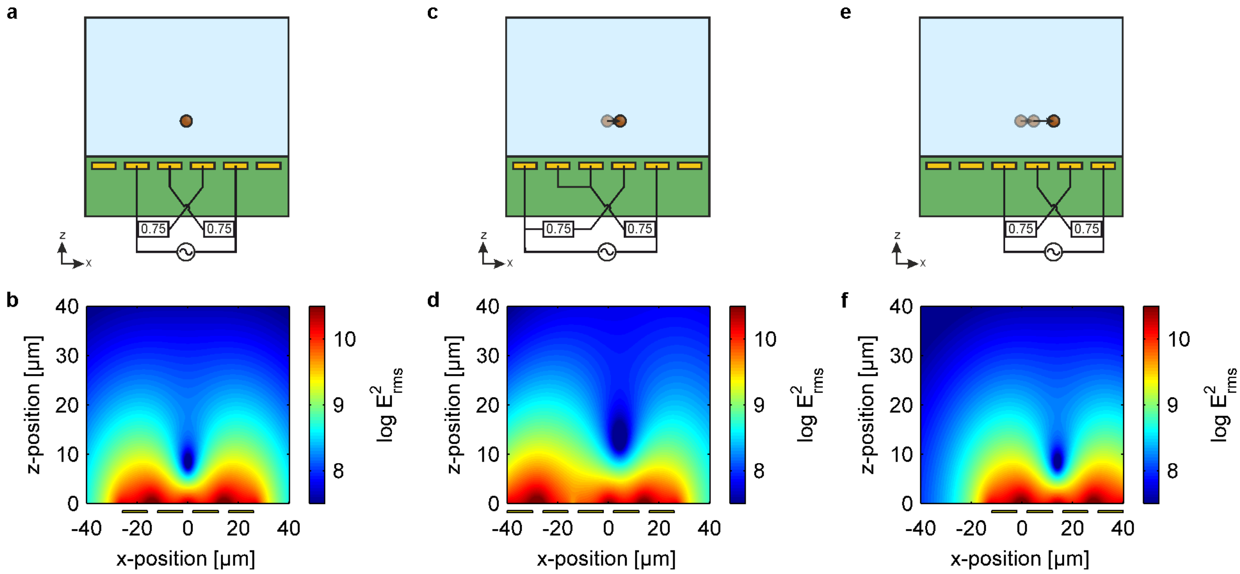

Figure S3: Schematics and simulated squared electric fields for the horizontal switching protocol with intermediate steps. **(a)** Applying AC signals with relative amplitudes of 1, -0.75, 0.7, and 1 can be used to trap a particle in the center of the four wires. **(b)** Simulated squared root-mean-square electric field for a peak-to-peak input voltage of $15\,\mathrm{V}$ applied as depicted in **(a)** (wire positions indicated by the yellow rectangles). **(c)** In order to relocate the particle to the right, an additional wire to the left of the particle is supplied with the AC signal of reduced amplitude. **(d)** Simulated squared root-mean-square electric field for the configuration shown in **(d)** for a peak-to-peak input voltage of $15\,\mathrm{V}$. The local minimum in the electric field is shifted towards the right and upwards. **(e)** and **(f)** Activating a configuration analogous to that in **(a)** but shifted by one wire completes the transfer of the particle.

3 Trap spacing below grid pitch

Using a magnetic trap, the geometry of the microwire array causes the peak in the magnetic field within a single trap to split into four side maxima. Figure S4 shows a simulation of a magnetic trap and its close vicinity, as well as the resulting particle distribution in the case of four trapped particles. The simulation was done with four wires each carrying a current of $I_0 = 100\,\mathrm{mA}$ in the direction indicated by the filled arrows. As can be seen in Figure S4b, each side maximum is occupied by an individual particle when four particles are placed in the trap[3]. When using wire arrays with a low interwire spacing, this effect can be used to generate closely spaced traps.

[3] P. Rinklin, RWTH Aachen, 2014.

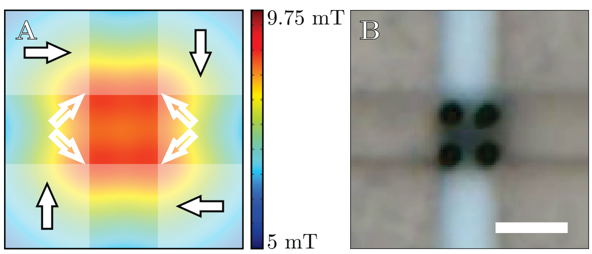

Figure S4: Simulated magnetic field and particle distribution illustrating closely spaced traps within a single cell of the array[3]. **(a)** Close-up of the simulated magnetic field in the central area of an active trap. The shaded regions indicate the edges of the surrounding four wires and the filled arrows indicate the current direction ($I_0 = 100\,\mathrm{mA}$ per wire). As marked by the empty arrows, the peak is composed of four side maxima. **(b)** Particle distribution for a group of four particles placed in a trap. As can be seen, all four particles occupy a different side maximum to minimize the magnetic potential energy. Scale bar: $10\,\mu\mathrm{m}$.

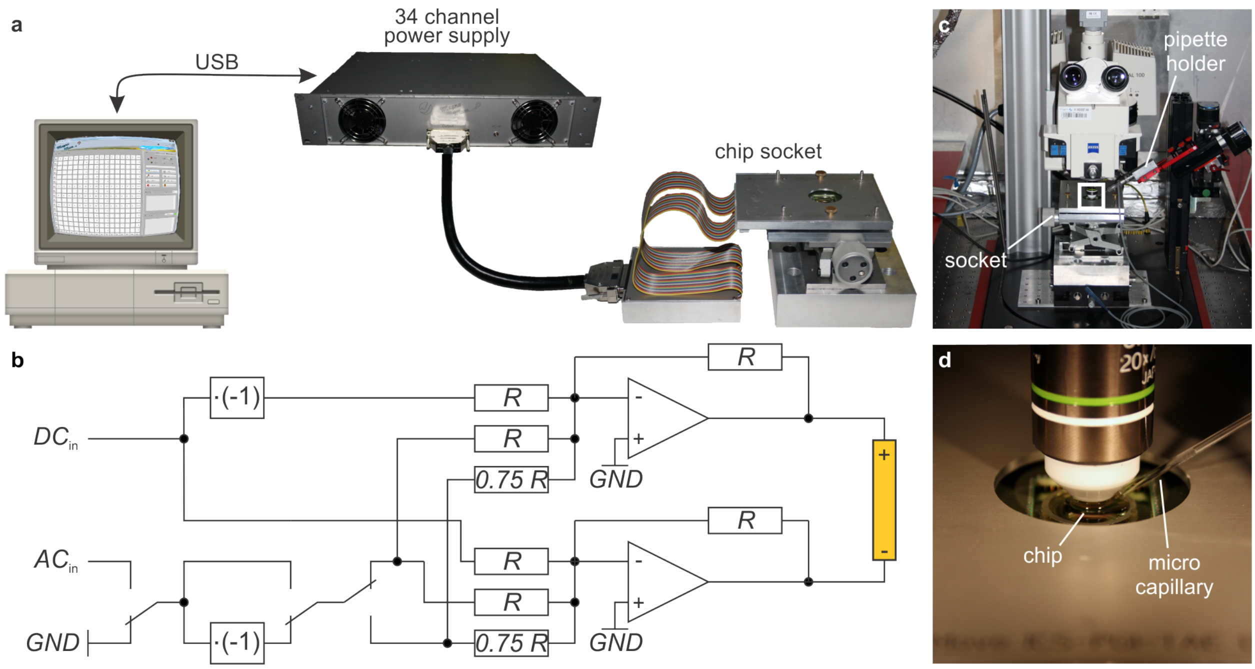

Figure S5: Power supply and setup used for three-dimensional particle control. **(a)** A custom-built power supply is controlled via a LabView software. The output signals are sent to a socket that is mounted to a z-table. **(b)** Schematic of the circuit of an individual channel. The DC voltage delivered by the micro controller is inverted while being routed to one end of the wire yielding an effective DC voltage of 2 DC_{in} over the wire. The AC signal from the external function generator can be inverted and/or multiplied with a factor of 0.75 before being applied to both ends of the wire. **(c)** and **(d)** The socket with the chip is mounted to the x/y-stage of the microscope and allows easy access with a pipette or a microcapillary.

4 Data analysis for particle tracking

In order to extract the particle's position from the video data recorded in the experiments, the following tracking routine was applied. First, the average of all frames of the data set was subtracted from the current frame. The result was multiplied with an amplification factor that was adjusted depending on video quality to obtain optimal results. The resulting frame was converted to a logical image using an intensity threshold of 201 of the 256 obtainable gray scale values. Subsequently, the frame was scanned for connected regions of pixels. These criteria were sufficient to correctly detect the region corresponding to the particle's position. The centroid of this region was then evaluated for its distance to the last known particle position. Depending on the frame rate of the video and the maximum expected velocity of the particle, a maximum step width between two successive frames was defined. The particle position was only noted if it followed this limit. Finally, the particle position was converted from pixels to micrometers using a scaling factor that was measured independently using the same optics. The absolute values of the particle's x- and y-position in the case of Figures 6b and 7 were shifted to arbitrary values for clarity.

5 Description of the setup

In order to exert three-dimensional control over individual microbeads on a chip, we used custom hard- and software components which will be described in the following. Figure S5a shows a general schematic of the electronic power supply and its control. A custom-built 34 channel power supply was controlled via a universal serial bus (USB) connection using a custom control software. This software allowed the control of the DC voltage applied to each of the 34 channels. The AC signals were generated by an external function generator (not shown) and were routed through the main power supply. Using the LabView software, the AC signals could be modified by factor of either 1, 0.75, -0.75, or -1. The final output signals were sent to a custom-built socket that was mounted on a z-table for height control. Figure S4:b shows a schematic of the circuit used to steer an individual wire. The wire is schematically depicted on the right as a yellow rectangle with both ends labelled with + and $-$. In order to apply an effective DC voltage DC_{eff} to a given wire, the microcontroller sends a voltage of $DC_{\text{in}} = {}^{DC_{\text{eff}}}/_{2}$ to the corresponding channel. This signal is then split and one half is inverted resulting in the desired effective DC voltage DC_{eff} being applied to the wire. In order to apply different AC signals to the wire, the AC input from the function generator (AC_{in}) can be either inverted or modified with a factor of 0.75. The result is then applied to both ends of the wire. Supplying two wires with ACin and AC_{in} thus resulted in an AC voltage of the same amplitude and frequency as AC_{in}. Figure S4:c and d show the custom socket mounted to the x/y-stage of the microscope setup, as well as a close up of the chip during an experiment, respectively. The custom socket was designed to allow easy access to the chip with a pipette or a microcapillary during the experiments.